RESEARCH ARTICLE

Molecular Nutrition & Food Research
www.mnf-journal.com

Short-Term Postnatal Overfeeding Induces Long-Lasting Cardiometabolic Syndrome in Mature and Old Mice Associated with Increased Sensitivity to Myocardial Infarction

*Eve Rigal, Marie Josse, Camille Greco, Nathalie Rosenblatt, Luc Rochette, Charles Guenancia, and Catherine Vergely**

Scope: Perinatal nutritional disturbances may "program" an increased cardio-metabolic risk in adulthood; however, few experimental studies have explored their effects on mature and/or old animal. This study aims to investigate the influence of postnatal overfeeding (PNOF) on cardiac function, sensitivity to ischemia-reperfusion (I-R) injury in vivo, glucose metabolism, and metabolic profile of pericardial adipose tissue (PAT) in young (4 months), adult (6 months), old (12 months), and very old (18 months) male mice.
Methods and results: Two days after birth, PNOF is induced by adjusting the litter size of C57BL/6 male mice to three pups/mother, while the normally fed (NF) control group is normalized to nine pups/mother. After weaning, all mice have free access to standard diet. Glucose/insulin tests and in vivo myocardial I-R injury are conducted on mice aged from 2 to 12 months, while echocardiography is performed at all ages up to 18 months. PNOF mice exhibit an early and persistent 10–20% increase in body weight and a 10% decrease in left ventricular ejection fraction throughout their lifespan. In PNOF mice aged 4, 6, and 12 months, glucose intolerance and insulin resistance are observed, as well as a 27–34% increase in infarct size. This is accompanied by a higher PAT mass with increased inflammatory status.
Conclusion: Short-term PNOF results in nutritional programming, inducing long-lasting alterations in glucose metabolism and cardiac vulnerability in male mice, lasting up to 12 months.

1. Introduction

Major risk factors of cardiovascular diseases in humans are related to aging, high blood pressure, glucose/insulin imbalance, dyslipidemia, overweight/obesity associated with visceral fat deposit. For instance, increased epicardial fat plays a role in the development of atrial fibrillation and cardiac fibrosis.[1,2] Preclinical models corresponding to the clinical features of metabolic syndrome are scarce, and the majority of experimental studies, including ours, were obtained in young male mice of 2–4 months old.

The nutritional environment during the perinatal period plays an essential role in permanently shaping gene expression in the fetus or new-born, which will be determinant in the subsequent orientation of an individual's cardiovascular and metabolic health.[3–6] This concept is generally referred to as the "Developmental Origins of Health and Disease" (DOHaD) and establishes a relationship between the perinatal

E. Rigal, M. Josse, C. Greco, L. Rochette, C. Guenancia, C. Vergely
Research Team: Physiopathologie et Epidémiologie Cérébro-Cardiovasculaires (PEC2)
Université de Bourgogne, Faculté des Sciences de Santé
7 Bd Jeanne d'Arc, Dijon 21000, France
E-mail: cvergely@u-bourgogne.fr

The ORCID identification number(s) for the author(s) of this article can be found under https://doi.org/10.1002/mnfr.202400136

DOI: 10.1002/mnfr.202400136

N. Rosenblatt
Division of Angiology
Heart and Vessel Department
Centre Hospitalier Universitaire Vaudois and University of Lausanne
Lausanne 1011, Switzerland

C. Guenancia
Cardiology Department
University Hospital of Dijon
Dijon 21000, France

environment and increased susceptibility to chronic diseases, introducing the concept of an individual being "programmed" to a certain phenotype in adulthood.[4,7–9] In this context, the impact of postnatal overfeeding (PNOF) can be explored in rodents with the model of litter size reduction.[10–13] Our research team and others have demonstrated that PNOF induced an early increase in body weight at weaning (+20–30%) that persisted during growth and maturity (6 months of age, +15–20%), and was associated with metabolic disorders, in particular abnormalities in glucose regulation and central adiposity.[14–16] Cardiac function was also impaired by PNOF: myocardial oxidative stress and collagen deposit were increased whereas a progressive decrease in left ventricular ejection fraction was observed in mice aged 6–7 months, and, ex vivo, the heart of PNOF mice was more sensitive to ischemia reperfusion (IR) injury.[13] However, young to adult PNOF rodents have often been used as a preclinical model to study the pathophysiology of metabolic syndrome in humans, which predominantly affects middle-aged to elderly patients, thereby limiting the clinical relevance.

Therefore, the aim of this study was to evaluate the long-term impact on cardiovascular system of a short-term PNOF, by assessing cardiac contractile function changes, in vivo cardiac sensitivity to ischemia-reperfusion injury and pericardial adipose tissue metabolic remodeling in young (4 months), adult (6 months), and mature (12 months) male mice.

2. Experimental Section

2.1. Ethics

All animals' procedures were reviewed and approved by the local ethics' committee (Comité d'Ethique en Expérimentation Animal, Université de Bourgogne Franche-Comté; protocol agreement number: 16589) and conformed to Directive 2010/63/EU of the European Parliament and to the Guide for the Care and Use of Laboratory Animals published by the US National Institutes of Health (NIH Publication No, 85–23, revised 1996). Animal welfare was the priority of all procedures to minimize the perceived suffering. For instance, their living environment had been enriched and animals were housed in groups.

2.2. Animals Model

Adult female C57BL/6J mice (Charles River, L'Arbresle, France) were paired with male C57BL/6J mice in individual cages during 1 week after which male mice were removed and the original groups of females reconstituted. Fifteen days after coupling, gravid females were isolated in individual cages for parturition. All animals received water and a standard pellet diet ad libitum during pregnancy and lactation. After delivery, on the second day of life, male pups were randomly distributed among the mothers to achieve cross fostering and the litter size was adjusted according to the study group: normal litters were composed of nine male pups leading to postnatally normally fed pups (NF groups) whereas postnatal overfed litter groups (PNOF groups) were reduced to three pups per mother (small litter). Excess pups were rapidly killed by decapitation. A total of 272 pups from 17 dams were used for this study. After weaning (day 24 of life, D24), mice of both groups had free access to a standard diet (A03, SAFE Diets Augy, France) and water. Throughout life, body weight was measured weekly then monthly up to 18 months of age. All weight data were collected from mice used in this project at different ages. Thus, mice aged 18 months were included in the average of weight values from previous ages.

2.3. Echocardiography

Transthoracic echocardiography was consecutively performed in 2, 4, 6, 12, and 18-month-old male mice, using the Vevo770 imaging system (VisualSonics Inc., Toronto, Canada), endowed with a 30 MHz probe.[17] Briefly, 41 NF and 41 PNOF mice were anesthetized with isoflurane and their body temperature was maintained at 37 ± 0.5 °C with an infrared lamp. The heart was imaged in the long-axis and short-axis view of the left ventricle (LV), with three measurements for each view to make an average. The cursor of the M mode was positioned perpendicular to the anterior wall to measure left ventricular end-diastolic and end-systolic diameters (LVEDD and LVESD, respectively) at the level of papillary muscles below the mitral valve tip. Heart rate and left ventricular ejection fraction (LVEF) were calculated[14] such as, E/A, E/e', and the ratio of the left ventricular mass on the body weight.

2.4. In Vivo Myocardial Ischemia Reperfusion

As previously described,[18,19] myocardial infarction was achieved by occlusion of the left anterior descending (LAD) coronary artery. Briefly, mice were anesthetized with isoflurane (4% then 2%) and placed under artificial ventilation with a specific mouse intubation cannula (outer diameter: 1.2 mm) before opening the chest. All incisions were preceded by the use of analgesic cream (Anesderm Ge, 5%). Once ventilated, a left thoracotomy wherein the pericardium was opened to expose the left ventricle was performed. The LAD coronary artery was ligated using 8.0 surgical thread for 45 min, in order to induce ischemic damage. Then, the slipknot was loosened to induce reperfusion. The chest was closed with 5.0 surgical thread and mice were awakened and placed in an incubator for better postsurgery recovery. All mice received two injections of buprenorphine (Buprecare, 0.075 mg kg^{-1}) to limit the pain. 24 h after the beginning of reperfusion, mice were anesthetized again, the chest was reopened and hearts were processed either for evaluation of infarct size, or for tissue sampling. Therefore, two separate sets of experiments were performed on different groups of mice to obtain results. Five mice per group were used at 2 months of age, and 12 mice per group were used for other ages to complete these surgical experiments.

2.5. Determination of Myocardial Area at Risk and Infarct Size

Twenty-four hours after reperfusion, in open-chest anesthetized mice, the LAD was re-occluded and the myocardial area at risk (AAR) was determined by injecting Evans blue (1%) in the bloodstream. All perfused tissues appeared stained in blue, except the

Table 1. Forward and reverse sequences of primers used for the amplification of mouse genes.

Primer name	Sense primer sequence	Antisens primer sequence
Actin β	5″-AGCTGCGTTTTACACCCTTT-3″	5″-AAGCCATGCCAATGTTGTCT-3″
Activin A	5″-GGGGAGAACGGGTATGTGGA-3″	5″-CCTGACTCGGCAAAGGTGAT-3″
IL-6	5″-CTGCAAGAGACTTCCATCCAG-3″	5″-AGTGGTATAGACAGGTCTGTTGG-3″
TNF α	5″-CAGGCGGTGCCTATGTCTC-3″	5″-CGATCACCCCGAAGTTCAGTAG-3″
STAT3	5″-CTTCAGACCCGCCAACA-3″	5″-TAGGACACTTTCTGCTGC-3″
Akt	5″-CCACGCTACTTCCTCCTC-3″	5″-CATCCTGAGGCCGTTCC-3″
ERK1	5″-GGTAGACCGTTCTGGAATG-3″	5″-GCAGAGCCCTACTCAGTG-3″
GSK3-β	5″-TGTTCTATGTGACTTGGTTTG-3″	5″-CAGAGTGGGAAGGGTGAA-3″
PI3K	5″-TTGTGGCGTCATAGATTGTGG-3″	5″-GTAACTTACCTAGCCCTTTGTGC-3″

AAR. The heart was quickly removed and was cut in 1 mm thick sections parallel to the sort axis of the left ventricle. A first acquisition of images was made to quantify the AAR, and then, the slices were incubated in 2% of Triphenyl Tetrazolium Chloride (TTC) at 37 °C for 20 min followed by 10% formalin for 45 min. A second round of images was performed to quantify the infarct size (IS), all images were treated with image J software. The AAR and the area corresponding to the IS were calculated as a percentage of the left ventricle.

2.6. Blood and Tissues Harvesting

Blood and tissue samples (pericardial adipose tissue [PAT], left ventricle) were collected for biological molecular experiments. Left ventricles were collected in intact mice, whereas PAT were harvested after cardiac surgery. All samples were stored in separate Eppendorf tubes, flash frozen in liquid nitrogen, and stored at −80 °C awaiting further experiments.

2.7. Glycemic Tests: ipGTT and ipITT

Intraperitoneal glucose tolerance tests (ipGTTs) and insulin tolerance tests (ipITTs) were carried out at 2, 4, 6, and 12 months of age, respectively, after 6 h of fasting. Blood glucose level was measured using a glucometer. As previously described[14] for GTTs, an intraperitoneal injection of glucose (2 g kg^{-1}) was administered, and blood droplets were collected twice from the tail vein just prior to glucose administration (time 0) and at 15, 30, 45, 60, 75, 90, 105, and 120 min following the injection. For ITTs, mice were injected with 0.75 IU kg^{-1} human recombinant insulin (Actrapid, Novo Nordisk, France) and blood glucose was determined at the same points as for the GTTs. Evolution of blood glucose was recorded for each group and at all ages and required a total of 72 mice, 9 mice per group per age without surgery protocol.

2.8. Real Time Quantitative Polymerase Chain Reactions (rt-qPCR)

Total RNA was extracted from frozen left ventricle and PAT samples by Nucleozol reagent (NucleoSpin RNA Set for NucleoZOL MACHEREY-NAGEL), mRNA (1 µg) was reverse transcribed with PrimeScript RT reagent Kit with gDNA Eraser (Takara). Real-time quantitative polymerase chain reaction (RT-qPCR) was performed with 2 µL of cDNA using the SYBR-Green PCR Master-Mix (Applied Biosystems) and both sense and antisense primers (5 mM) in a final volume of 20 µL, in a StepOne-Real-Time PCR system (Applied Biosystems). The primers used for the amplification of mouse genes were provided in **Table 1**. Data were analyzed using relative quantification, normalized against actin beta mRNA as the house keeping gene and presented as fold change compared to 4 months NF mice sample.

2.9. Western Blot Analysis

Heart tissues without cardiac surgery were lysed using the Precellys homogenizer combined with the Cryolys module (Bertin Technologies) and zirconium beads (ZROB10, Next Advance) in 10 volumes of radioimmunoprecipitation assay (R0278, Sigma-Aldrich) buffer containing protease and phosphatase inhibitors (A32961, ThermoFisher) at 4 °C. The homogenates were then centrifuged during 15 min at 10 000 × *g* at 4 °C to separate proteins from cell debris, and the protein concentration in the supernatant was measured using the Lowry method.

Equal protein amounts were loaded and separated on a sodium dodecyl sulfate-polyacrilamide gel electrophoresis (SDS-PAGE) using the TGX Stain-Free FasctCast Acrylamide kit (1610175, Biorad) under reducing and denaturing conditions. Proteins were then transferred to polyvinylidene difluoride (PVDF) membrane using Turbo Transblot technology. After blocking nonspecific binding site with 5% nonfat milk for total AKT and with 7.5% bovine albumin serum in 0.1% PBS/Tween 20 for phosphorylated AKT (AKT-P on Ser473) during 1 h at room temperature (RT), membranes were incubated 2 h at 4 °C with primary antibodies against total AKT (4691, Cell signaling) and AKT-P (4060, Cell signaling). The membranes were washed three times for 5 min with 0.1% PBS/Tween 20 and then incubated for 1 h at RT with antirabbit IgG HRP-linked secondary antibody (7074, Cell signaling). Detection of antibody reactivity was performed with WesterbRight Sirius Substrate (K-12043, Advansta) using the Chemidoc imaging system (Biorad). Each revealed band was normalized to the total amount of protein loaded on the corresponding lane, as determined by the stain-free technology. Gels were run in duplicate and chemoluminescence measurements were analyzed with Image Lab Software (Biorad).

2.10. ELISA Quantification of Activin A

The activin A homodimer was measured by ELISA (R&D systems, DAC00B) in a 3-step quantitative sandwich enzyme immunoassay technique. Briefly, the capture antibody was biotinylated and bound to streptavidin-coated plates. The plates were washed, and assay diluent, standards, and samples were pipetted into the wells and any activities A present was bound by the immobilized antibody. After washing away any unbound substances, an HRP-conjugate specific for the βA subunit was added to each well. Following a wash to remove any unbound conjugate, a substrate solution was added to the wells and color developed in proportion to the amount of activin A bound. The color development was stopped, and the intensity of the color was measured at 450 nm. The mean sensitivity was 3.67 pg mL^{-1}. The mean intra- and inter assay coefficients of variation (CV) of the assay were 4.3% and 5.9%, respectively. This quantification was carried out on plasma from mice that underwent the cardiac surgery protocol.

2.11. Luminex Discovery Assay: Interleukin 6, Tumor Necrosis Factor α, and Interleukin 1β

The study used mouse premixed multianalyte kit (LXSAMSM) to simultaneous detect some inflammation biomarkers in mice plasma. Analyte-specific antibodies (IL-6, TNF-α, and IL-1β) were precoated onto magnetic microparticles fixed with fluorophores at set ratios for each unique bead region. Microparticles, standards, and samples were added into wells and the immobilized antibodies bound the analytes of interest. The unbound substances were eliminated by washing and a biotinylated antibody cocktail specific to the analytes of interest was pipetted to each well. Following a wash to remove any unbound biotinylated antibody, streptavidin-phycoerythrin conjugate (Streptavidin-PE), which binds to the biotinylated antibody, was added to each well. Final washes removed unbound streptavidin-PE, the microparticles were resuspended in buffer and read using the Bio-Rad Bio-Plex analyzer. Bio-Rad Bio-Plex used one laser to excite the dyes inside each bead to identify the bead region and the second laser to excite the PE to measure the amount of analyte bound to the bead. All fluorescence emissions from each bead as it passed through the flow cell were then analyzed to differentiate emission levels using a Photomultiplier Tube (PMT) and an Avalanche Photodiode. This quantification was realized on plasma from mice that underwent the cardiac surgery protocol.

2.12. Mouse/Rat GDF-15 Immunoassay

This assay used the quantitative sandwich enzyme immunoassay technique (MGD150, Bio-Techne). A monoclonal antibody specific for mouse/rat GDF-15 had been precoated onto a microplate. Standards, control, and samples were incubated into the wells for 2 h at room temperature (RT) and any GDF-15 present was bound to the immobilized antibody. After washing away any unbound substances, a primary mouse/rat GDF-15 antibody conjugated to horseradish peroxidase was added to the wells and incubated for an additional 2 h at RT. Following a wash to remove any unbound antibody-enzyme reagent, a substrate solution composed of hydrogen peroxide and tetramethylbenzidine was pipetted to the wells. The enzyme reaction showed a blue product that turned yellow when the stop solution (hydrochloric acid) was added. The intensity of the color measured by spectrophotometer VICTOR3 (Perkin Elmer) at 450 nm was in proportion to the amount of GDF-15 bound in the initial step. The sample values were then read off the standard curve. This quantification was carried out on plasma from mice that underwent the cardiac surgery protocol.

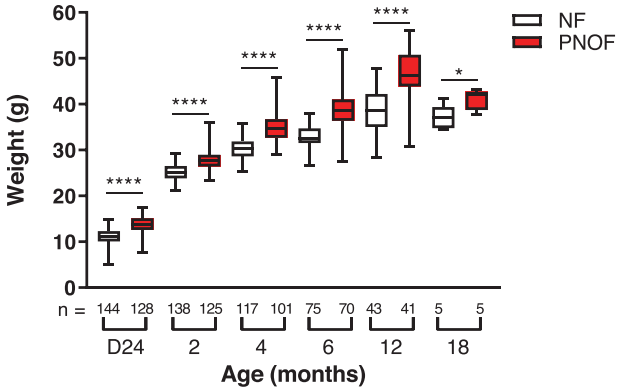

Figure 1. Evolution of body weight in postnatally normally fed (NF) and overfed (PNOF) mice from 24 days up to 18 months of age. Results are expressed as median ± min to max values, *: $p < 0.05$ was considered significantly different (one-way ANOVA), ***: $p < 0.001$. All mice used for this project are presented. Thus, 18-month-old mice are included in all previous datapoints.

2.13. Statistical Analysis

Data were presented as mean ± standard error of mean (SEM) for glucose tests and biomolecular analysis and as medians ± min to max values for body weight, LVEF evolution, and for cardiac quantification of AAR and IS. To compare NF and PNOF means in same age group, a Student's *t*-test was used (PAT weight). A one-way ANOVA followed by Tukey's test was used to compare groups over time (LVEF, plasma markers, body weight, rt-qPCR, and Western blot). To compare the effect of age and group, a two-way ANOVA followed by Tukey's test was used (glucose tests and IL-6, PI3K, and GSK3β mRNA). Statistical significance was set at $p < 0.05$. The data were analyzed using GraphPadPrism.

3. Results

3.1. PNOF Induced Early and Permanent Increase in Body Weight

PNOF induced early and permanent increase in body weight (**Figure 1**). At weaning (D24), the body weight of PNOF group was 20% greater than the NF group ($p < 0001$). This difference persisted in juvenile ($p < 0.001$), young ($p < 0.001$), adult ($p < 0.001$), mature ($p < 0.001$), and even in old mice ($p < 0.05$).

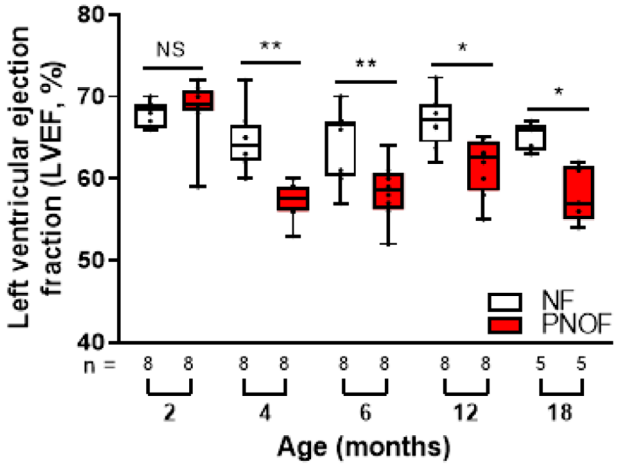

Figure 2. Left ventricular ejection fraction (LVEF, %) in postnatally normally fed (NF) and overfed (PNOF) mice from 2 to 18 months of age. The numbers (*n*) are listed by age for the two groups. LVEF was calculated by measuring the left ventricular internal diameter in the end diastolic and end systolic by echocardiography (VEVO 770, Visualsonics). Data are expressed as medians ± min to max values. *p* was calculated by one-way ANOVA, *: $p < 0.05$, **: $p < 0.01$.

3.2. PNOF Induced Early and Permanent Decrease in Cardiac Contractile Function

Consecutive echocardiographic measurements showed an alteration of left ventricular contractile function in PNOF mice from 4 months up to 18 months of age, with an average LVEF decrease of −9% to −11% for PNOF males compared to NF groups (**Figure 2**). We did not observe any alterations of other parameters accounting for LV dimensions, systolic or diastolic function (**Table 2**).

3.3. PNOF Induced Increased Susceptibility to Myocardial Ischemia-Reperfusion Injury In Vivo

After an in vivo 45-min cardiac ischemia followed by 24 h of reperfusion, the area at risk (AAR) was similar in all groups at all ages, which allowed us to rigorously compare the results concerning infarct sizes (**Figure 3A**). We observed a significant increase of the infarct size in hearts of PNOF group in mice aged 4 months (+27%, $p < 0.05$), 6 months (+34%, $p < 0.001$), and 12 months (+27%, $p < 0.05$) as compared to the NF group (Figure 3B) but not in mice aged 2 months.

3.4. PNOF Induced Early and Permanent Alteration in Glucose and Insulin Tolerance

At 2, 4, 6, and 12 months of age, glucose and insulin tolerance tests were performed in mice after 6 h of fasting. For ipGTT test, all PNOF mice (12 months) presented greater glycemia after intraperitoneal injection of glucose compared to NF group, as evidenced by higher incremental areas mean under the curve of glycemia during the experiments (near +15% at 2 [$p < 0.05$], 4 [$p < 0.05$], 6 [$p < 0.01$], and +32% at 12 months [$p < 0.01$]). For ipITT test, the area mean under curve of PNOF group was lower in 4-, 6-, and 12-month-old mice compared to the NF group (respectively −14%, $p < 0.05$, −26%, $p < 0.05$, and −37%, $p < 0.05$) (**Figure 4**). We also observed a transient higher fasting glycemia in the PNOF group mice as compared to the NF, but only at 6 months of age (data not shown, $p < 0.001$).

3.5. PNOF Induced Increase in Pericardial Adipose Tissue Mass and Inflammatory Status

The pericardial adipose tissue (PAT) weight was adjusted to body weight. In PNOF mice, the pericardial fat mass was higher at 6 (+30%, $p < 0.01$) and 12 months of age (+25%, $p < 0.001$) as compared to the NF group (**Figure 5A**).

Gene expression of Activin A in pericardial adipose tissue was decreased in the PNOF group compared to the NF group at 12 months (−56%, $p < 0.05$), and a nonsignificant trend to decrease over time was found in PNOF mice (−41% from 4 to 12 months, $p = 0.413$) (Figure 5B).

Gene expression of TNF-α in pericardial fat mass was increased in PNOF group at 4 (+40%, $p < 0.05$) and 12 months (+76%, $p < 0.05$) as compared to the NF group (Figure 5D). Moreover, IL-6 gene expression was also increased with time in the PNOF group (+99% from 4 to 12 months, $p < 0.05$) and was significantly higher in PNOF group at 12 months (+84%, $p < 0.05$) (Figure 5C).

Table 2. Echocardiographic parameters from postnatally normally fed (NF) and overfed (PNOF) mice of 4, 6, 12, and 18 months of age.

	4 months		6 months		12 months		18 months	
	NF mean ± SEM	PNOF mean ± SEM	NF mean ± SEM	PNOF mean ± SEM	NF mean ± SEM	PNOF mean ± SEM	NF mean ± SEM	PNOF mean ± SEM
LVIDd [mm]	3.91 ± 0.67	4.11 ± 0.05	4.16 ± 0.12	4.26 ± 0.15	4.12 ± 0.10	4.21 ± 0.13	4.18 ± 0.12	4.40 ± 0.12
Heart rate [beats min^{-1}]	432 ± 11.8	445 ± 13.7	492 ± 25.7	480 ± 19.8	472 ± 11.9	507 ± 9.1	442 ± 16.3	460 ± 10.9
E/A	1.41 ± 0.04	1.34 ± 0.05	1.57 ± 0.07	1.48 ± 0.05	1.61 ± 0.04	1.49 ± 0.07	1.52 ± 0.09	1.39 ± 0.06
E/e´	36.9 ± 2.50	35.0 ± 1.34	25.7 ± 1.67	21.5 ± 1.73	27.1 ± 2.93	31.8 ± 3.29	21.4 ± 2.48	27.5 ± 4.05
LV mass/body weight	4.31 ± 0.11	4.53 ± 0.11	4.20 ± 0.23	3.99 ± 0.25	3.50 ± 0.26	3.55 ± 0.24	3.98 ± 0.46	3.86 ± 0.15

Acquisition was made using the VEVO 770 imaging system (Visualsonics) with a 30 MHz probe. *A*, late diastolic transmitral flow velocities; *e'*, peak early-diastolic annular velocities; *E*, early diastolic transmitral flow velocities; LVEF, left ventricular ejection fraction; LVIDd, diastolic left ventricular internal diameters. *p* was calculated by one-way ANOVA test. *: $p < 0.05$, **$p < 0.01$; ****: $p < 0.0001$: significantly different from NF group.

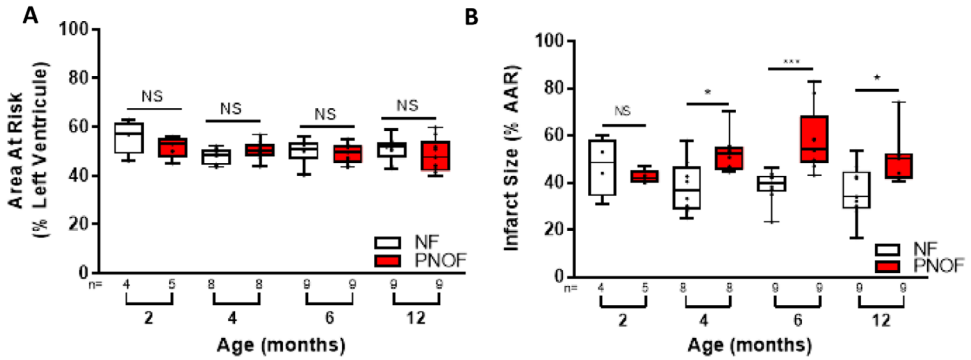

Figure 3. Quantification of area at risk (AAR, A) and infarct size (IS, B) in hearts of postnatally normally fed (NF) and overfed (PNOF) mice of 4–12 months of age after in vivo ischemia (45 min) induced by ligation of LAD coronary artery followed by 24 h of reperfusion. The AAR was quantified by Evan's blue coloration and the IS using Triphenyl Tetrazolium Chloride staining. All experiments required a minimum of one set of animals for each age group, with 8–12 mice per group. The images were treated using image J software. Data are expressed as medians ± min to max values, p was calculated by one-way ANOVA, within the same age, *: $p < 0.05$, ***: $p < 0.001$.

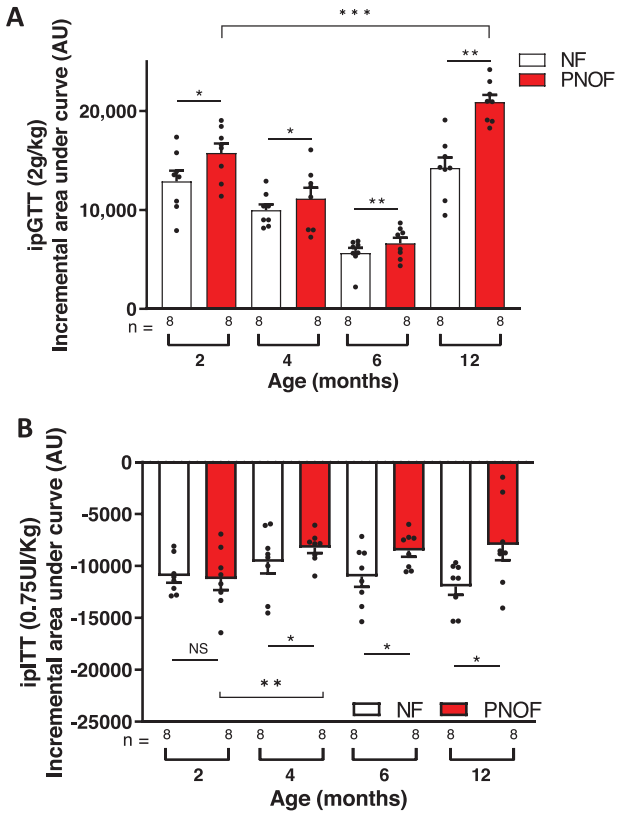

Figure 4. Evaluation of glucose metabolism in postnatally normally fed (NF) and overfed (PNOF) mice of 2–12 months of age. Incremental area under the curve of blood glucose after intraperitoneal glucose (A) or insulin injection (B) in NF and PNOF mice (8 mice per group). Incremental area under curve was determined by subtracting the mean basal blood glucose value from the mean of duplicate blood glucose value obtained at each measurement time for each mouse, and histogram represents the additional area at each timepoint. All mice participated in ipGTT followed by ipITT 1 week later. Data are expressed as means ± SEM. p was calculated by two-way ANOVA test, *: $p < 0.05$, **: $p < 0.01$, ***: $p < 0.001$.

3.6. PNOF Induced Alterations in the Expression of Genes Involved in Cardioprotection

Concerning the cardioprotective RISK pathway (**Figure** 6A–E), at 4 months, we observed a 58% decrease of PI3K gene expression ($p < 0.05$), −30% for Akt ($p < 0.001$), −32% for ERK1 ($p < 0.001$), −40% for eNOS ($p < 0.01$), and a trend to decrease for GSK3-β ($p = 0.114$) and, in hearts of 6-months-old PNOF mice, a 23% decrease in Akt gene expression ($p < 0.05$), and a 35% decrease in ERK1 expression ($p < 0.01$). At 12 months, we observed a 44% decrease of Akt gene expression ($p < 0.05$) and −51% for ERK1 ($p < 0.01$), −25% for eNOS ($p < 0.01$) in PNOF hearts compared to NF. Additionally, at 12 months, a reduced phosphorylation of Akt protein was observed in ventricular tissue of PNOF mice (Figure 6G), revealing lower activation. We also observed a 75% increase of PI3K and GSK3-β gene expression between 4 and 12 months in PNOF mice's hearts. Concerning SAFE pathways, the gene expression of STAT3 was reduced by 30% in 4 ($p < 0.001$) and 6 months-($p < 0.01$) old PNOF mice hearts and by 69% at 12 months (Figure 6F).

3.7. PNOF Moderately Increased Circulating Markers of Inflammation

After cardiac ischemia reperfusion, the plasma concentration of activin A was similar in our two study groups at all ages, even if there was a tendency to increase in PNOF at 4 months as compared to NF mice ($p = 0.067$, **Table** 3). Plasma concentration of activin A changed over time in PNOF, and, at 12 months, it was significantly lower than at 4 months, with a decrease of 70% ($p < 0.05$).

Blood concentrations of TNF-α and IL-1β were undetectable in our samples. Blood concentration of IL-6 trend to increase in the PNOF mice at 4 months, and this increase became significant at 6 months ($p < 0.05$) compared to NF group after cardiac IR.

Finally, we observed no difference in our groups for GDF-15 plasma concentration after the in vivo myocardial surgery (Table 3).

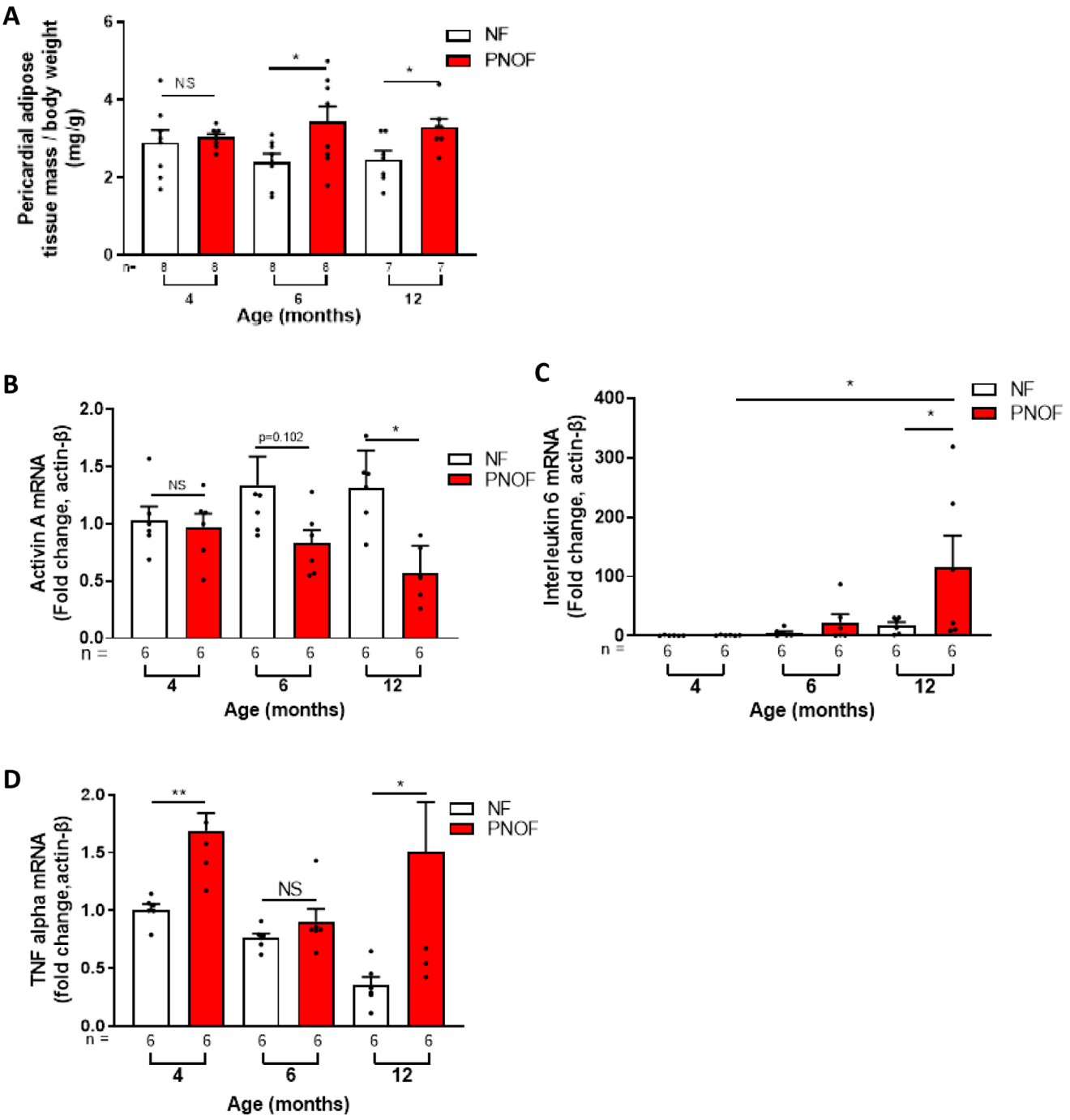

Figure 5. Mass of the pericardial fat and (A) quantitative rt-qPCR analysis for activin A (B), IL-6 (C), and TNF-α (D) in pericardial adipose tissue (PAT) of postnatally normally fed (NF) and overfed (PNOF) mice of 4–12 months of age. The pericardial adipose tissue mass was weighted after tissue harvesting after the cardiac ischemia-reperfusion protocol. RNAs were extracted from PAT after harvesting. Data are expressed as the fold change relative to the beta actin gene expression. Experiments were carried out in singlicate. Data are expressed as means ± SEM, p was calculated by student's t-test, within the same age for the comparison of PAT mass, and by one-way ANOVA test for rt-qPCR or by two-way ANOVA for study changes over time. *: $p < 0.05$, **: $p < 0.01$, ***: $p < 0.001$.

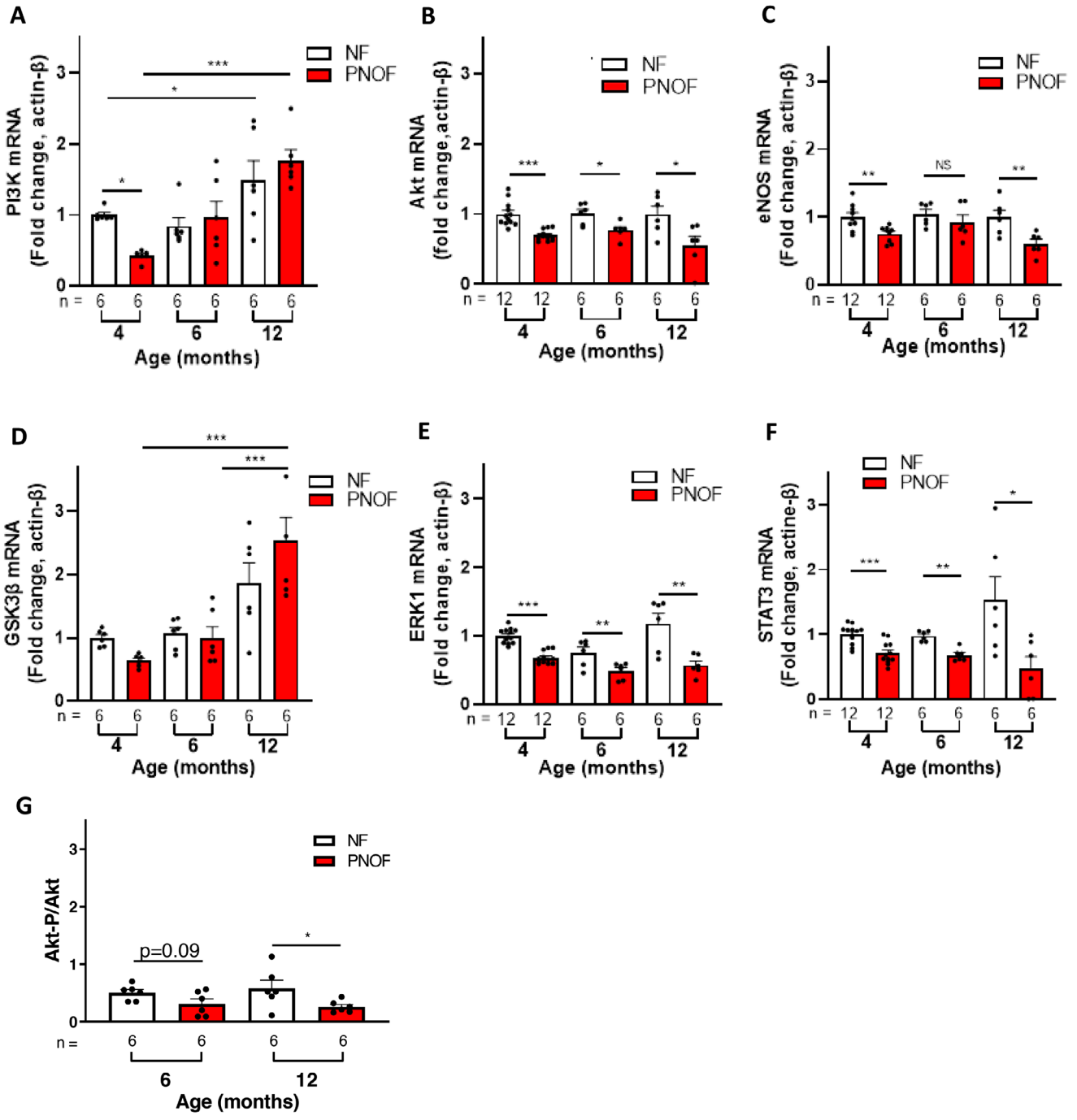

Figure 6. Quantitative rt-qPCR analysis for PI3K (A), Akt (B), eNOS (C), GSK3-β(D), ERK1 (E), and STAT3 (F) in left ventricle of postnatally normally fed (NF) and overfed (PNOF) mice of 4, 6, and 12 months of age. Western Blot for total AKT and its phosphorylated form in left ventricle of postnatally normally fed (NF) and overfed (PNOF) mice of 6 and 12 months of age (G). RNAs and proteins were extracted from total left ventricle after harvesting. For RT q-PCR, data are expressed as the fold change relative to the beta actin gene expression and represents the mean ± SEM. For Western Blot, the phosphorylated form of AKT was reported to its nonphosphorylated total form. Experiments were carried out in singlicate. p was calculated by one-way ANOVA test: *: $p < 0.05$, **: $p < 0.01$, ***: $p < 0.0001$.

4. Discussion

Postnatal overfeeding (PNOF) is a well-established model for studying perinatally programmed overweight and other pathophysiological disturbances.[10] Considering that 2 days after birth pups were mixed and randomly distributed among mothers in small or large litters, the differences observed might not be attributed to distinct ancestors.

Our study provides new and original data concerning a permanent programming effect of PNOF on the cardiovascular

Table 3. Circulating plasma concentration of Activin A, IL-6, and GDF-15 in postnatally normally fed (NF) and overfed (PNOF) mice, 24 h after in vivo myocardial ischemia reperfusion.

	4 months		6 months		12 months	
	NF mean ± SEM	PNOF mean ± SEM	NF mean ± SEM	PNOF mean ± SEM	NF mean ± SEM	PNOF mean ± SEM
Activin A [pg mL^{-1}]	102.2 ± 30.69	234.4 ± 52.56	120.2 ± 43.75	93.84 ± 31.09	77.05 ± 14.75	70.39 ± 13.92$^{\#}$
IL-6 [pg mL^{-1}]	106.5 ± 41.12	293.6 ± 130.6	16.04 ± 3.60	163.1 ± 55.32*	55.37 ± 26.98	91.22 ± 60.50
GDF-15 [pg mL^{-1}]	181.9 ± 15.79	217.0 ± 61.85	188.4 ± 25.74	285.4 ± 56.48	260.0 ± 43.62	389.7 ± 29.14

Results are obtained in thawed mice plasma. The amount of TNF-α and IL-1β were undetectable (not shown). p was calculated by one-way ANOVA test, $^{*}p < 0.05$: significantly different from NF group same age; $^{\#}p < 0.05$, 12 months different to 4 months in the same group.

and metabolism system of mature to very old mice. The alteration induced by PNOF from the weaning still impacts the cardiometabolic system until 18 months of life in mice.

PNOF mice developed an early overweight observable from weaning at 24 days of life which persisted throughout growth, maturation, and even senescence (until 18 months of age). These results are consistent with those already found by our team and others,[20] which observed an increase in food intake of nearly 15–20% per day and a rise of body fat mass at the expense of lean mass.[14] The increase of food intake has been related to changes in hypothalamic expression of orexigenic and anorexigenic neuropeptides.[21] Other experimental studies demonstrated that, at weaning, PNOF mice[22] and rats[23,24] presented visceral and subcutaneous fat accumulation with increased adipocyte surface,[16,25,26] whereas in adult PNOF mice only an increase in visceral fat was present, a situation which is in favor of a "central adiposity concept."

We show that cardiac contractile function was also decreased by PNOF in young (4 months), adult (6 months), mature (12 months), and for the first time, in very old (18 months) mice with a nearly 10% reduction in LVEF. Therefore, this decrease in LV contractility is mild, and should not be considered as relevant for heart failure with reduced ejection fraction (HFrEF). Our results also suggest that only the systolic not the diastolic function was impacted by PNOF. Additionally, we did not observe any cardiac hypertrophy evaluated either through heart to body mass or to heart mass to tibial length. On the contrary, other authors found that PNOF induced cardiac hypertrophy in mice or in rats,[14,17,27,28] but these differences could be explained by the echocardiographic method of measurement. Interestingly, we noticed that the modification of cardiac function appeared between 2 and 4 months of age, suggesting that before 2 months, the heart of PNOF mice was able to adapt its function to maintain normal LVEF, despite the early changes induced in the myocardium by PNOF. In fact, previous studies from our team have shown early modification of cardiac gene expression impacting isoforms of actin, myosin, collagen, and other structural proteins.[17] Later on, other circulating or local environmental factors like myocardial oxidative stress or increased leptin blood levels might also play a role in a cardiac remodeling phenomenon.[29–31]

PNOF leads to a greater sensitivity to in vivo myocardial ischemia that may be observed from 4-month-old young mice and up to 12 months after birth. These results corroborate previous data from our team, showing a higher sensitivity of isolated perfused hearts to ischemia in PNOF mice aged 7 months, showing lower functional parameters recovery and a higher infarct size after 30 min of global ischemia.[17] This increased heart sensitivity to both in vivo and ex vivo ischemia reperfusion could be explained in part by the alterations of cardioprotective pathways, especially for SAFE, which may predispose the heart to a greater damage during ischemic processes. In fact, in left ventricles of nonischemic hearts from 4-month-old PNOF mice, our original data show a decrease both in PI3K, Akt, eNOS and ERK1 (RISK pathway),[32] and in STAT3 (SAFE pathways).[33] At 12 months, while the PCR results regarding RISK pathway may not offer conclusive findings, the Western blot analysis indicates an alteration in AKT activation. This modification suggests a potential reduction in RISK pathway activation, associated with diminished gene activation of the SAFE pathway induced by PNOF. The exact mechanism of this programming needs further exploration and may involve epigenetic processes such as gene methylation,[34] histone modifications or interfering RNAs.[35] Additionally, this long-lasting increased vulnerability to ischemia could also involve other molecular pathways such as oxidative stress and inflammation.

It is admitted that an impairment of glucose or lipid metabolism has an impact on cardiovascular function.[36,37] Indeed, in previous studies originating from our lab, we showed increased plasma levels of cholesterol, insulin, and leptin, associated with glucose metabolism alterations in 6-month-old PNOF mice.[17] Some of these criteria belong to the definition of metabolic syndrome and were also described in other studies.[13,38,39] In the present work, we performed an extensive study of glucose metabolism in young (2 months) to mature 12-month-old male mice. We found that PNOF induced early glucose intolerance from the 2nd month of life and an insulin resistance from the 4th month of life that persistent to 12 months. This altered glycemic status evolve over time since they are more severe with age and could explain altered cardiac function and higher sensitivity to myocardial infarction.[40] In PNOF swiss mice, other research teams have found a diminution of phosphorylated Akt1 and PI3K-Irs1,[38] both involved in insulin signaling pathways, which may have a direct impact in the ischemic heart. Moreover, it was shown that, from weaning[41] to adulthood,[23] PNOF mice presented hyperglycemia and hyperinsulinemia related to elevated GLUT2 content in pancreatic islets leading to increased insulin secretion.[23] Additionally, PNOF mice exhibit

changes in peripheral insulin signaling, like downregulation of insulin receptor substrate-1 (Irs-1) and glucose transporter 4 (GLUT4) in white adipose tissue and skeletal muscle,[42,43] reducing glucose uptake and reinforcing the insulin resistance phenotype in these mice.[44]

Interestingly, in this study, we observed that adult and old PNOF mice have increased pericardial fat mass, which displays a greater inflammatory status highlighted by an increase in gene expression of TNF-α and IL-6. In clinical studies, the volumes of epicardial and pericardial adipose tissues (EAT and PAT) are correlated with obesity, metabolic syndrome, insulin resistance, leptin level, and diabetes.[45] Our findings concerning PAT strengthen the similarity of our original experimental model to the characteristics of metabolic syndrome described in humans. It is well known that EAT has paracrine effect on the myocardium which might not be such documented for PAT. By both paracrine and endocrine effect, PAT could communicate with the myocardium and influence its inflammatory status and cardiac function. It was also speculated that activin A originating from the EAT would exert direct profibrotic effect in the myocardium inducing the expression of TGF-β1 and β2 in rat atria.[1] Histological studies from our team showed a higher collagen density in biopsies of adult PNOF mice ventricle, associated with a local oxidative stress.[17] However, in this study, activin A gene expression in PAT and its plasma concentration were not increased at any age in PNOF group. Instead, activin A mRNA expression in PAT of PNOF aged 12 months old was decreased, and plasma concentration decreased over time. Most research support the notion that activin A has deleterious effects on the heart, but one study has shown that the overexpression of activin A can protect myocytes from cardiac stress both in vivo and in vitro.[46] In our study, the reduction of activin A mRNA expression in PAT could promote higher cardiac sensitivity to IR in PNOF mice. In addition, in our model, the fibrosis status is probably not related to activin A but could rather be due to an oxidative status of ventricle, as we described earlier,[17] and could be enhanced by the proinflammatory status of PAT.

This study has certain limitation, including the use of only male animals and the exclusion of females. The decision to use only males was based on the potential cardiovascular protection induced by estrogens in females. Consequently, a separate study focusing exclusively on female individuals is planned to address this gender-specific aspect.

In conclusion, our results highlighted the programming effect of overnutrition during the immediate postnatal period on cardio-metabolic function in young, adult, mature, and old male mice. From weaning, PNOF mice developed overweight that modified body composition in favor of visceral and pericardial fat mass, associated with alterations of systolic cardiac function, higher sensitivity to ischemia reperfusion injury induced in vivo and abnormal glucose metabolism. Therefore, this experimental model of PNOF can be considered as original and significantly relevant to the main characteristics of metabolic syndrome as described in humans. Interestingly, all these modifications appear very soon in life, from 4 months of age and persist with time, up to 12 months of age. Intriguingly, only 21 days of PNOF are sufficient to modify permanently the long-term health and impact both the cardiac and the metabolic function. More studies are needed to explore the exact pathways involved in programming phenomenon, but it should be emphasized that adjusting litter size in rodent's group may be a necessary prerequisite in experimental procedures aimed at evaluating cardiometabolic function.

Acknowledgements

The authors gratefully thank Ivan Porcherot and Sandy Guner for technical assistance. This work was supported by grants from the French Ministry of Research, the Regional Council of Burgundy, the Association de Cardiologie de Bourgogne (ACB), the E2S doctoral school of Dijon, the Fondation de France, and the Fédération Française de Cardiologie.

Conflict of Interest

The authors declare no conflict of interest.

Author Contributions

Study conception and design: C.V., C.G. Acquisition of data: E.R., M.J. Analysis and interpretation of data: E.R., C.V., C.G., N.R., L.R. Drafting of manuscript: E.R., C.V., C.G., N.R.

Keywords

insulin resistance, ischemia-reperfusion injury, metabolic syndrome, pericardial adipose tissue, postnatal programming

Received: February 21, 2024
Revised: May 28, 2024
Published online: June 27, 2024

[1] N. Venteclef, V. Guglielmi, E. Balse, B. Gaborit, A. Cotillard, F. Atassi, J. Amour, P. Leprince, A. Dutour, K. Clément, S. N Hatem, *Eur. Heart J.* **2015**, *36*, 795.
[2] B. Gaborit, N. Venteclef, P. Ancel, V. Pelloux, V. Gariboldi, P. Leprince, J. Amour, S N. Hatem, E. Jouve, A. Dutour, K. Clément, *Cardiovasc. Res.* **2015**, *108*, 62.
[3] Z. Ye, Y. Huang, D. Liu, X. Chen, D. Wang, D. Huang, Li Zhao, X. Xiao, *PLoS One* **2012**, *7*, e47013.
[4] S. C. Langley-Evans, *Proc. Nutr. Soc.* **2006**, *65*, 97.
[5] P. Zhang, D. Zhu, Y. Zhang, L. Li, X. Chen, W. Zhang, R. Shi, J. Tao, B. Han, Z. Xu, *Mol. Nutr. Food Res.* **2018**, *62*, 1700771.
[6] R. Obeid, S. J. P. M. Eussen, M. Mommers, L. Smits, C. Thijs, *Mol. Nutr. Food Res.* **2022**, *66*, e2100662.
[7] O. J. Carpinello, A. H. DeCherney, M. J. Hill, *Semin. Reprod. Med.* **2018**, *36*, 177.
[8] D. J. P. Barker, *J. Epidemiol. Community Health* **2004**, *58*, 114.
[9] M. Agoudemos, B. E. Reinking, S. L. Koppenhafer, J. L. Segar, T. D. Scholz, *Neonatology* **2011**, *100*, 198.
[10] M. Parra-Vargas, M. Ramon-Krauel, C. Lerin, J. C. Jimenez-Chillaron, *Cell Metab.* **2020**, *32*, 334.
[11] M. Josse, E. Rigal, N. Rosenblatt-Velin, L. Rochette, et al., *Int. J. Mol. Sci.* **2020**, 21.
[12] A. Plagemann, I. Heidrich, F. Götz, W. Rohde, G. Dörner, *Exp. Clin. Endocrinol.* **1992**, *99*, 154.
[13] A. Habbout, S. Delemasure, F. Goirand, J.-C. Guilland, F. Chabod, M. Sediki, L. Rochette, C. Vergely, *Biochimie* **2012**, *94*, 117.
[14] N. Li, C. Guenancia, E. Rigal, O. Hachet, et al., *Sci. Rep.* **2016**, *6*, 30817.

[15] T. Harder, A. Rake, W. Rohde, G. Doerner, A. Plagemann, *Endocr. Regul.* **1999**, *33*, 25.
[16] S. Boullu-Ciocca, A. Dutour, V. Guillaume, V. Achard, C. Oliver, M. Grino, *Diabetes* **2005**, *54*, 197.
[17] A. Habbout, C. Guenancia, J. Lorin, E. Rigal, C. Fassot, L. Rochette, C. Vergely, *PLoS One* **2013**, *8*, e56981.
[18] F. Huet, J. Fauconnier, M. Legall, P. Sicard, C. Lozza, A. Lacampagne, F. Roubille, *Future Sci. OA* **2020**, *7*, FSO656.
[19] E. Belaidi, A. Thomas, G. Bourdier, S. Moulin, E. Lemarié, P. Levy, J.-L. Pépin, I. Korichneva, D. Godin-Ribuot, C. Arnaud, *Int. J. Cardiol.* **2016**, *210*, 45.
[20] A. Plagemann, *Horm. Res.* **2006**, *65*, 83.
[21] H. Davidowa, Y. Li, A. Plagemann, *Eur. J. Neurosci.* **2003**, *18*, 613.
[22] M. M. Glavas, M. A. Kirigiti, X. Q. Xiao, P. J. Enriori, et al., *Endocrinology* **2010**, *151*, 1598.
[23] A. C. De Souza Rodrigues Cunha, R. O. Pereira, M. J. Dos Santos Pereira, V. De Melo Soares, M. R. Martins, M. Teixeira Teixeira, É. P. G. Souza, A. S. Moura, *J. Nutr. Biochem.* **2009**, *20*, 435.
[24] D. Muñoz-Valverde, P. Rodríguez-Rodríguez, P. Y. Gutierrez-Arzapalo, A. L. López De Pablo, M. Carmen González, R. López-Giménez, B. Somoza, S. M. Arribas, *Physiol. Res.* **2015**, *64*, 547.
[25] S. Boullu-Ciocca, V. Achard, V. Tassistro, A. Dutour, M. Grino, *Diabetes* **2008**, *57*, 669.
[26] M. Hou, Y. Liu, L. Zhu, B. Sun, M. Guo, J. Burén, X. Li, *PLoS One* **2011**, *6*, e25726.
[27] A. S B Moreira, M. Teixeira Teixeira, F. Da Silveira Osso, R. O Pereira, G. De Oliveira Silva-Junior, E. P. Garcia De Souza, C. A. Mandarim De Lacerda, A. S Moura, *Nutr. Metab. Cardiovasc. Dis.* **2009**, *19*, 805.
[28] M. D. F. Junior, K. V. N. Cavalcante, L. A. Ferreira, P. R. Lopes, C. N. R. Pontes, A De Sá M De Bessa, Â. R. Neves, F. A. Francisco, G. R. Pedrino, C. H. Xavier, P C De F Mathias, C. H De Castro, R. M. Gomes, *Life Sci.* **2019**, *226*, 173.
[29] M. Lopez, L. M. Seoane, S. Tovar, M. C. Garcia, R. Nogueiras, C. Diéguez, R. M. Señarís, *Diabetologia* **2005**, *48*, 140.
[30] E. Velkoska, T. J. Cole, M. J. Morris, *Am. J. Physiol. Endocrinol. Metab.* **2005**, *288*, E1236.
[31] A. L. Rodrigues, E. G. De Moura, M. C. F. Passos, I. H. Trevenzoli, E. P. S. Da Conceição, I. T. Bonono, J. F. N. Neto, P. C. Lisboa, *J. Nutr. Biochem.* **2011**, *22*, 109.
[32] V. Sivaraman, N. R. Mudalgiri, C. Salvo, S. Kolvekar, M. Hayward, J. Yap, B. Keogh, D. J. Hausenloy, D. M Yellon, *Basic Res. Cardiol.* **2007**, *102*, 453.
[33] R F. Kelly, K T. Lamont, S. Somers, D. Hacking, L. Lacerda, P. Thomas, L H. Opie, S. Lecour, *Basic Res. Cardiol.* **2010**, *105*, 763.
[34] A. Plagemann, T. Harder, M. Brunn, A. Harder, K. Roepke, M. Wittrock-Staar, T. Ziska, K. Schellong, E. Rodekamp, K. Melchior, J W. Dudenhausen, *J. Physiol.* **2009**, *587*, 4963.
[35] B. Siddeek, N. Li, C. Mauduit, H. Chehade, E. Rigal, J.-F. Tolsa, J.-B. Armengaud, C. Yzydorczyk, M. Benahmed, C. Vergely, U. Simeoni, *Nutr. Metab. Cardiovasc. Dis.* **2018**, *28*, 944.
[36] O. G. Kolterman, R. S. Gray, J. Griffin, P. Burstein, J. Insel, J. A. Scarlett, J. M. Olefsky, *J. Clin. Invest.* **1981**, *68*, 957.
[37] K. M. Godfrey, D Jp Barker, *Am. J. Clin. Nutr.* **2000**, *71*, 1344SS.
[38] M. R. Martins, A. K. G. Vieira, É. P. G. De Souza, A. S. Moura, *J. Endocrinol.* **2008**, *198*, 591.
[39] L. L. Souza, E. G. Moura, P. C. Lisboa, *Nutrients* **2022**, *14*, 2045.
[40] K. Shinlapawittayatorn, S C. Chattipakorn, N. Chattipakorn, *Curr. Med. Chem.* **2018**, *25*, 1501.
[41] Q. Du, H. Hosoda, T. Umekawa, T. Kinouchi, N. Ito, M. Miyazato, K. Kangawa, T. Ikeda, *Peptides* **2015**, *70*, 23.
[42] H.-W. Liu, S. Mahmood, M. Srinivasan, D J. Smiraglia, M S. Patel, *J. Nutr. Biochem.* **2013**, *24*, 1859.
[43] F. Bei, J. Jia, Yi-Q Jia, J.-H. Sun, F. Liang, Z-Yi Yu, W. Cai, *Lipids Health Dis.* **2015**, *14*, 96.
[44] A. L. Rodrigues, É. P. G. De Souza, S. V. Da Silva, D. S. B. Rodrigues, A. B. Nascimento, C. Barja-Fidalgo, M. S. De Freitas, *J. Endocrinol.* **2007**, *195*, 485.
[45] G. Lazaros, A. Antonopoulos, C. Antoniades, D. Tousoulis, *Curr. Cardiol. Rep.* **2018**, *20*, 40.
[46] Y. Oshima, N. Ouchi, M. Shimano, D. R. Pimentel, et al., *Circulation* **2009**, *120*, 1606.